Thermodynamic Modeling Suggests Declines in Water Uptake and Acidity of Inorganic Aerosols in Beijing Winter Haze Events during 2014/2015–2018/2019

Thermodynamic Modeling Suggests Declines in Water Uptake and Acidity of Inorganic Aerosols in Beijing Winter Haze Events during 2014/2015–2018/2019

Shaojie Song,[†,‡] Athanasios Nenes,[§,£] Meng Gao,[‡] Yuzhong Zhang,[‡] Pengfei Liu,[‡] Jingyuan Shao,[⊥] Dechao Ye,[†] Weiqi Xu,[#] Lu Lei,[#] Yele Sun,[#,*] Baoxian Liu,[†,∥,*] Shuxiao Wang,[†,*] Michael B. McElroy[‡]

[†]School of Environment, Tsinghua University, Beijing 100084, China

[‡]School of Engineering and Applied Sciences, Harvard University, Cambridge, Massachusetts 02138, USA

[§]School of Architecture, Civil and Environmental Engineering, Ecole Polytechnique Fédérale de Lausanne, CH-1015, Lausanne, Switzerland

[£]Institute for Chemical Engineering Sciences, Foundation for Research and Technology Hellas, Patras, GR-26504, Greece

[⊥]School of Physics, Peking University, Beijing 100871, China

[#]State Key Laboratory of Atmospheric Boundary Physics and Atmospheric Chemistry, Institute of Atmospheric Physics, Chinese Academy of Sciences, Beijing 100029, China

[∥]Beijing Key Laboratory of Airborne Particulate Matter Monitoring Technology, Beijing Municipal Environmental Monitoring Center, Beijing 100048, China

ABSTRACT

During recent years, aggressive air pollution mitigation measures in northern China have resulted in considerable changes in gas and aerosol chemical composition. But it is unclear whether aerosol water content and acidity respond to these changes. The two parameters have been shown to affect heterogenous production of winter haze aerosols. Here, we performed thermodynamic equilibrium modeling using chemical and meteorological data observed in urban Beijing for four recent winter seasons and quantified the changes in the mass growth factor and pH of inorganic aerosols. We focused on high relative humidity (> 60%) conditions when submicron particles have been shown to be in the liquid state. From 2014/2015 to 2018/2019, the modeled mass growth factor decreased by about 9%–17% due to changes in aerosol compositions (more nitrate and less sulfate and

chloride) and the modeled pH increased by about 0.3–0.4 unit mainly due to rising ammonia. A buffer equation is derived from semivolatile ammonia partitioning, which helps understand the sensitivity of pH to meteorological and chemical variables. The findings provide implications for evaluating the potential chemical feedback in secondary aerosol production and the effectiveness of ammonia control as a measure to alleviate winter haze.

1. INTRODUCTION

One ubiquitous component of ambient aerosols is condensed water, which partitions to particles from water vapor.[1] The abundance of aerosol-phase water primarily depends on relative humidity (RH), particle mass, and chemical composition.[2] Aerosol water contributes to aerosol mass,[3] alters physical properties,[4,5] facilitates gas-to-particle uptake of semivolatile species,[6] and provides the medium for heterogeneous (multiphase) processes.[7-9] Studies have suggested that aerosol water plays a role in the formation of northern China winter haze, a serious public health issue.[10-13] A positive feedback mechanism has been proposed,[12] in which aerosol water promotes secondary aerosol production and the product aerosols, in turn, enhance water uptake. Aerosol water content and acidity (or pH) are considered as two influencing parameters, with the first representing the space for heterogeneous processes and the second determining rates of many chemical reactions.[14-18] Hence, it is useful to characterize these two parameters for understanding haze formation.

A general approach to measuring aerosol water content is by perturbing RH and detecting the changes in aerosol physical properties, e.g., using nephelometers or hygroscopicity tandem differential mobility analyzers,[3,19,20] but such measurements are not performed routinely in China. Another common approach involves thermodynamic equilibrium analyses between gas and aerosol phase for semivolatile species, requiring composition measurements and a thermodynamic model (e.g., E-AIM or ISORROPIA).[2,21,22] Intercomparisons indicate that water contents estimated

from the two approaches are in good agreement.[3,12,23] Thermodynamic analyses on the basis of gaseous and aerosol compositions are also considered as the best available method to estimate the pH of ambient aerosols.[24] Direct pH measurement techniques developed in the laboratory are difficult to apply in ambient air.[25,26] Over the past few years, dozens of studies have examined the water content and acidity of northern China winter haze aerosols using thermodynamic models.[10-12,27-36] Major findings include: aerosol water content, mainly contributed by uptake of inorganic components, increases rapidly with haze accumulation due to enhancement of both particle mass and RH; and aqueous aerosols are moderately acidic (average pH of about 4 to 5) primarily due to abundant ammonia.

Stringent anthropogenic emission controls, especially since implementation of the China Clean Air Action Plan in 2013, have led to considerable changes in aerosol loadings and chemical compositions as well as in the levels of reactive gases.[37-42] For example, the annual mean concentrations of fine particles decreased by about 50% over the North China Plain during 2013–2018, according to the national monitoring network.[43] The question arises, but remains unanswered, as to how the water content and acidity of aerosols have responded to these changes. Quantifying their responses is helpful for evaluating potential feedbacks associated with secondary aerosol production. Here, we conduct thermodynamic analyses using high-time-resolution data observed in Beijing for four winter seasons from 2014/2015 to 2018/2019. To our knowledge, this is the first attempt to address the questions highlighted here for this region, although the sensitivity of aerosol acidity to changes in chemical compositions has been studied in other areas, e.g., North America.[44-49]

2. MATERIALS AND METHODS

Field campaigns in four winter seasons (2014/2015, 2016/2017, 2017/2018, and 2018/2019) were conducted in urban Beijing. Meteorological variables (temperature and RH), gaseous ammonia, and chemical components of non-refractory submicron particles (NR-PM_1) including organics, sulfate, nitrate, ammonium, and chloride, were measured at time resolutions < 5 minutes. Details (sampling dates and location, instrumentation, and uncertainty quantification) are provided in the Supporting Information (SI). Measured chemical species and meteorological parameters served as inputs to the ISORROPIA II thermodynamic equilibrium model for calculating the water content and pH of inorganic aerosols (pH_i).[21,50] Here, pH_i was defined as the molality-based hydrogen ion activity on a logarithmic scale, following the recommendation by the International Union of Pure and Applied Chemistry (IUPAC),[51]

$$\mathrm{pH_i} = -\log_{10}\left(a_{\mathrm{H^+_{(aq)}}}\right) = -\log_{10}\left(m_{\mathrm{H^+_{(aq)}}}\gamma_{\mathrm{H^+_{(aq)}}}/m^{\Theta}\right) \quad (1)$$

where $a_{\mathrm{H^+_{(aq)}}}$ is hydrogen ion activity in aqueous solution, $\mathrm{H^+_{(aq)}}$. $m_{\mathrm{H^+_{(aq)}}}$ and $\gamma_{\mathrm{H^+_{(aq)}}}$ are the molality and the molality-based activity coefficient of $\mathrm{H^+_{(aq)}}$, respectively. $m^{\Theta} = 1\ \mathrm{mol\ kg^{-1}}$ is the standard molality. The model inputs were averaged on an hourly basis for consistency with the timescales for semivolatile species to reach equilibrium.[52] Only inorganic aerosol species (i.e., sulfate, nitrate, ammonium, and chloride) were included in our calculations, since inorganics and organics were expected to reside in separate liquid phases for Beijing winter haze. The average oxygen-to-carbon (O/C) elemental ratios were observed to be < 0.5,[53] and studies have shown that liquid-liquid phase separation of organic–inorganic mixtures occurs almost always when O/C < 0.5.[24,54,55] It should be noted that hydrophilic organic acid salts (e.g., oxalate) may reside in the same phase with inorganic ions, but unfortunately they were not measured in this study. We thus conducted a

sensitivity calculation to evaluate the potential influence of their presence on the modeled acidity and water uptake. Another drawback in our measurements was not including non-volatile cations, and we conducted another sensitivity calculation to evaluate their possible effect.

The most recent ISORROPIA model v2.3 was used with the pH algorithmic issue fixed.[33] The pH solution procedure has been described in Song et al. (2018).[33] Because the amount of aerosol water is much smaller than that of water vapor in the atmosphere, the model assumes that aerosol water uptake does not change ambient RH.[1] In addition, the model does not consider the effect of surface tension on equilibrium droplet radii, which may be important for aerosols with radii less than about 50 nm.[56] Given these assumptions, phase equilibrium shows that aerosol water activity (a_w) equals to RH. Aerosol water content (AWC) in ISORROPIA is estimated with the Zdanovskii-Stokes-Robinson (ZSR) mixing rule,[57,58] linking water uptake of a multicomponent aerosol to that of the individual electrolytes,

$$\mathrm{AWC} = \sum_i \frac{M_i}{m_{oi}(a_w)} \tag{2}$$

where AWC is the total water concentration (kg m^{-3}), M_i is the molar concentration of electrolyte i (mol m^{-3}) and is solved iteratively in the model, and $m_{oi}(a_w)$ is the molality (mol kg^{-1}) of a binary solution of electrolyte i at a given a_w. $m_{oi}(a_w)$ is specified in ISORROPIA using outputs from the model E-AIM III. Although based on semi-ideality, the ZSR rule has been shown to provide a good prediction of water uptake and widely used in aerosol models.[59-62] The mass growth factor for inorganic aerosols, G_{mi}, was computed as Equation (3) using the AWC (kg m^{-3}) and dry aerosol concentration (m_{i}, kg m^{-3}) calculated using the ISORROPIA model and measured chemical species and meteorological parameters.

$$G_{\mathrm{mi}} = \frac{\mathrm{AWC} + m_{\mathrm{i}}}{m_{\mathrm{i}}} \quad (3)$$

Here, we exported the contribution of each electrolyte to the total AWC from ISORROPIA, in order to evaluate the effect of aerosol composition changes. The forward mode (using total chemical measurements as inputs) was adopted in this work, since the reverse mode (using only particle data as inputs) is strongly affected by errors in particle measurements.[63] The calculations were made assuming both stable and metastable thermodynamic equilibrium states, with the stable assuming that solids precipitate when RH is below the deliquescence RH and the metastable assuming that aerosols may constitute a supersaturated solution at low RH. We used a Monte Carlo approach to propagate measurement uncertainties to model predictions (more information in SI).[33] The measured and predicted gaseous NH_3 concentrations agreed reasonably well, indicating good model behavior (Figure S1).

Our thermodynamic model calculations were conducted mainly using ISORROPIA because of its high computational efficiency (allowing for uncertainty quantification using the Monte Carlo approach) and because of the availability of its source code (allowing for model development to evaluate the relative contributions of different electrolytes to aerosol water uptake). But since it is developed for large-scale atmospheric models, ISORROPIA is subject to many simplifications.[21] Thus, we also conducted thermodynamic calculations using a benchmark model E-AIM IV.[64]

3. RESULTS AND DISCUSSION

Figure 1 shows mass fractions of NR-PM_1 chemical components for four winter seasons including also a comparison of aerosol compositions under low and high RH conditions. A RH of 60% was chosen as the dividing line since the particle physical state transitions from the semisolid to liquid state when ambient RH increases above this value.[14] Similar to previous studies,[12,65,66] we found

that the mass fractions of sulfate increased by 50%–130% at high RH compared with low RH conditions, which had been hypothesized to arise from sulfate production in aerosol water through different chemical pathways.[10,11,67,68] Dissolved $SO_{2(aq)}$ (the sum of $SO_2 \cdot H_2O$, HSO_3^-, and SO_3^{2-}) has been suggested to be oxidized in aerosol water by NO_2, H_2O_2, and O_2 catalyzed by transition metal ions (Fe^{3+} and Mn^{2+}). The higher RH resulted in an increase in aerosol water content, which provided a larger volume for heterogeneous reactions to occur. From 2014/2015 to 2018/2019, the mass fractions of nitrate increased by a factor of about 1.5. Nitrate has replaced sulfate as the most abundant inorganic component,[40] a circumstance that may be attributed to the faster decline of emissions of SO_2 relative to NO_x in Beijing and surrounding areas.[38,43] The mass fractions of organics and chloride were reduced, likely due to the substantial decreases in coal and biomass combustions.[38,42,53,69]

Figure 1 also shows that the mass concentrations of PM_1 varied significantly among different winters. The average PM_1 concentrations in 2017/2018 winter (46 μg m^{-3} at high RH) were much lower compared with the other winter seasons (from 139 to 222 μg m^{-3} at high RH). Several studies (using chemical transport models or statistical models) have investigated the influences of reduced emissions and meteorology on PM concentrations in Beijing for recent years.[43,70,71] They generally suggested a major role of emission and a minor role of meteorology. Cheng N. et al. (2019)[70] found, different from the other seasons, that wintertime $PM_{2.5}$ did not decrease significantly (on a 90% confidence level) during 2013–2016 due to unfavorable meteorological conditions. Cheng J. et al. (2019)[71] showed that $PM_{2.5}$ mass concentrations in 2017/2018 winter would increase by about 80% if the meteorological conditions were the same with 2016/2017 winter, although there was a negative bias in the modeled $PM_{2.5}$ compared to observations in 2016/2017. More stringent emission control measures, including the suspension of industrial activities and the replacement of

167 coal with natural gas, were implemented in 2017/2018 winter over Beijing and surrounding regions
168 in order to meet the target of $PM_{2.5}$ concentration for the 2013–2017 Clean Air Action Plan, and
169 were suggested to significantly reduce PM concentrations during this winter season.[72] In this study,
170 G_{mi} was used to evaluate the response of inorganic aerosol water uptake to the changes in the mass
171 fractions of aerosol components. It was considered a better metric for such a purpose than AWC
172 since it was primarily affected by mass fractions of chemical species rather than aerosol dry mass,
173 which varied among different haze events as described above.
174

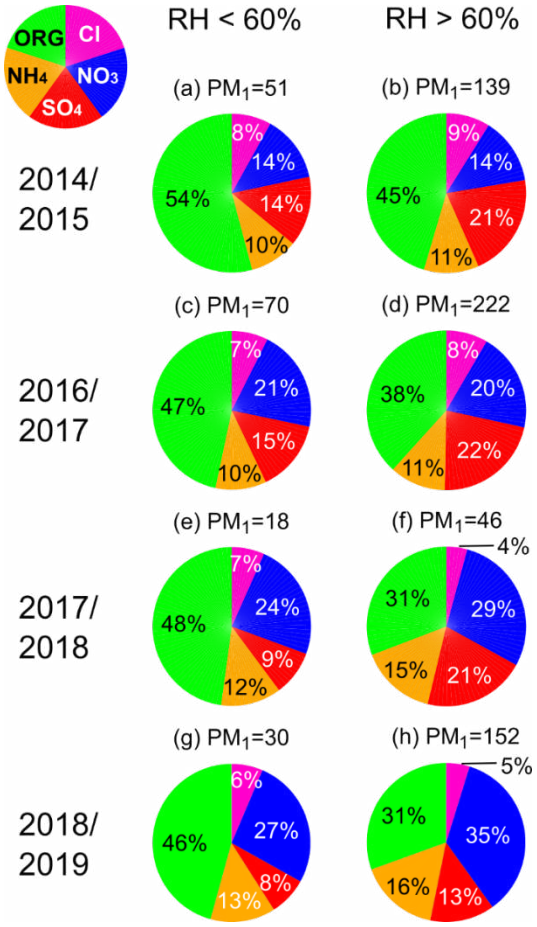

175

176 Figure 1. Mean mass fractions of NR-PM_1 chemical components at low (< 60%) and high (> 60%)
177 RH conditions. (a–b), (c–d), (e–f), and (g–h) present data for the winters of 2014/2015, 2016/2017,

178 2017/2018, and 2018/2019, respectively. The unit of PM_1 concentration is μg m^{-3}. ORG, NH_4,
179 SO_4, NO_3, and Cl represent organics, ammonium, sulfate, nitrate, and chloride, respectively.
180
181 Figure 2(a) shows the modeled G_{mi} in winter 2014/2015 as a function of RH. Ambient aerosols
182 could exist in either stable or metastable equilibrium state, depending on their compositions and
183 RH experience,[73] but there has not been enough evidence to demonstrate the state of Beijing winter
184 aerosols.[33] As we expect, G_{mi} increased from 1.0 to about 3.0 when RH increased from 17% to
185 83%. The metastable G_{mi} showed a monotonic increase with RH, while the stable G_{mi} remained at
186 1.0 below RH of about 50% (the mutual deliquescence RH). G_{mi} in both states converged when
187 RH reached 75% as all inorganic salts deliquesced. As shown in Figure 2(b–c), the modeled G_{mi}
188 in the following winter seasons decreased relative to 2014/2015, regardless of state assumptions.
189 The amplitudes for G_{mi} decline increased with RH, reaching 3% ± 3%, 10% ± 3%, and 13% ± 4%
190 in 2016/2017, 2017/2018, and 2018/2019, respectively.
191
192 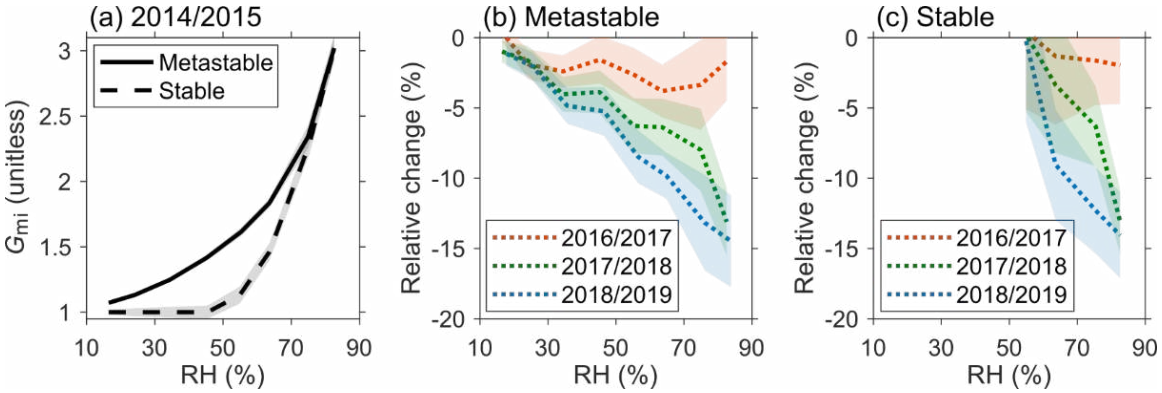

193 Figure 2. (a) shows inorganic aerosol mass growth factors (G_{mi}) for the 2014/2015 winter as a
194 function of RH modeled using both metastable and stable assumptions. (b–c) show the relative G_{mi}
195 changes in the winters of 2016/2017, 2017/2018 and 2018/2019 as compared to 2014/2015. Data
196 are grouped in RH bins (10% increment). The shaded areas indicate the 1σ uncertainty range.

We show next that the modeled declining water-uptake ability resulted from changed inorganic aerosol compositions. Figure 3(a–c) present the contribution of each electrolyte ($(NH_4)_2SO_4$, NH_4NO_3, and NH_4Cl) to the total AWC. Note that the AWC calculation followed the ZSR rule and that almost all sulfate existed in the form of $(NH_4)_2SO_4$. Figure 3(d) shows the amount of water uptake per electrolyte on a mass basis. Note that $(NH_4)_2SO_4$ and NH_4Cl are subject to efflorescence at RH of above 30% and extending the curves to lower RH may not be realistic for these pure salts.[74] Ambient particles consisting of multiple salts exhibit a more complex behavior in efflorescence RH. The curves in Figure 3(d) are thus used only to demonstrate the different water-uptake ability of each electrolyte. Among the three electrolytes, $(NH_4)_2SO_4$ showed the highest ability and NH_4NO_3 the lowest. We found, below 30% RH, that most water uptake could be attributed to $(NH_4)_2SO_4$. At high RH, all three electrolytes contributed significantly. The importance of NH_4Cl has often been ignored in previous studies. The contribution of NH_4NO_3 increased from < 20% in 2014/2015 to > 50% in 2018/2019, whereas the contributions of both $(NH_4)_2SO_4$ and NH_4Cl decreased over the same period. During recent years, the relative increase and low water-uptake ability of NH_4NO_3 have resulted in a 9%–17% decline of the modeled G_{mi} during winter haze events (Figure 2). As mentioned in METHODS, ISORROPIA uses the output data from E-AIM model III[75] to specify the amount of water uptake for each electrolyte. It should be noted that for NH_4NO_3 and $(NH_4)_2SO_4$ the water-uptake data in E-AIM III are different from those in E-AIM model II[76] and IV[64] (these two versions have very similar data) when RH is below about 50% (Figure S2). A recalculation using the water-uptake data from E-AIM IV shows, when RH is below 50%, a higher contribution of NH_4NO_3 and a lower contribution of $(NH_4)_2SO_4$ to the total AWC (Figure S3). As this study was focused on winter haze conditions associated with high

RH, the difference in water uptake between different thermodynamic models did not change our main findings.

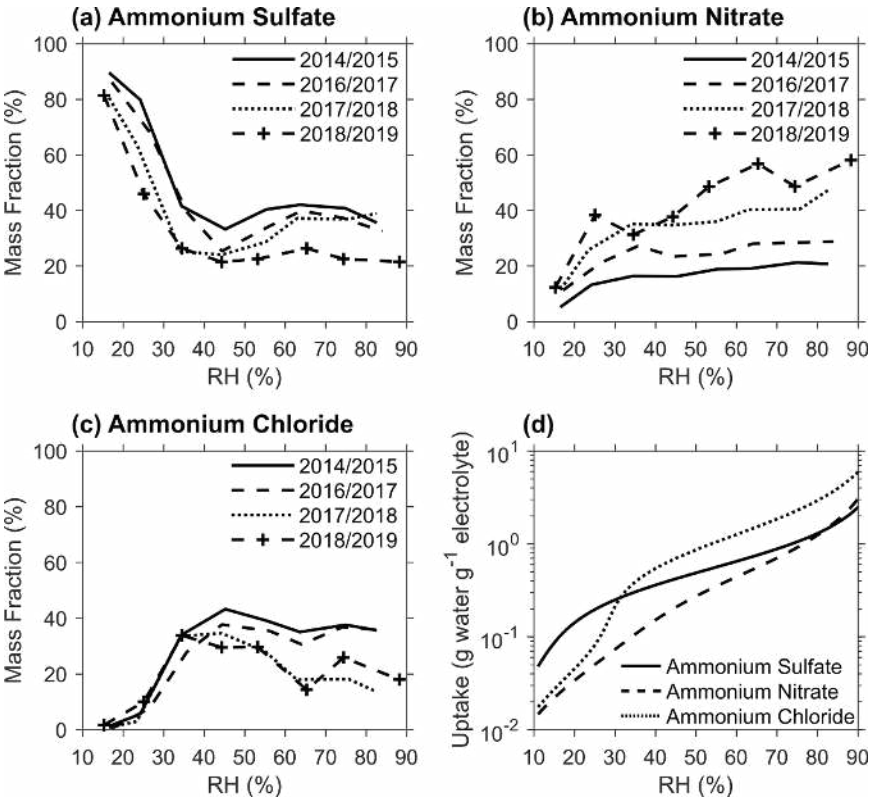

Figure 3. (a–c) show the modeled mass fractions of aerosol water content associated with different electrolytes. (d) shows the amount of water uptake per mass of each electrolyte in a binary solution. Data are presented as a function of RH. Data in (a–c) are calculated based on field measurements and ISORROPIA and grouped in RH bins (10% increment). Data in (d) are obtained from ISORROPIA.

pH_i of Beijing haze aerosols has been suggested to be buffered by abundant ammonia in the gas phase.[32-34] Under such condition, the partitioning of nitric acid ($HNO_{3(g)} \leftrightarrow H^+_{(aq)} + NO^-_{3(aq)}$) and hydrochloric acid ($HCl_{(g)} \leftrightarrow H^+_{(aq)} + Cl^-_{(aq)}$) was strongly shifted toward the aerosol phase,

and thus both $[HNO_{3(g)}]$ and $[HCl_{(g)}]$ were very low,[32,33] suggesting that they did not strongly buffer pH_i. We derive the buffer equation from phase equilibrium of $NH_{3(g)} + H^+_{(aq)} \leftrightarrow NH^+_{4(aq)}$ (details in the SI), similar to the Henderson–Hasselbalch equation,[77]

$$pH_i = pK^* + \log_{10}\left(\frac{[NH_{3(g)}]}{a_{NH^+_{4(aq)}}}\right) \quad (4)$$

where K^* (μmol m^{-3}) is the apparent equilibrium constant, $[NH_{3(g)}]$ (μmol m^{-3}) is gaseous NH_3 molar concentration, and $a_{NH^+_{4(aq)}}(\text{mol kg}^{-1}) = [NH^+_{4(aq)}]\gamma_{NH^+_{4(aq)}}$ is the molality-based activity of $NH^+_{4(aq)}$. Equation (4) suggests that pH_i is affected by three variables: pK^*, $[NH_{3(g)}]$, and $a_{NH^+_{4(aq)}}$. pK^* depends only on T and decreases by about 0.05 unit per K increase. This dependence reflects the relationships of both ammonia solubility and water dissociation with T. $\log_{10}([NH_{3(g)}])$ indicates about a 1 unit increase in pH_i per 10-fold increase in $[NH_{3(g)}]$, consistent with earlier results from Guo et al. (2017).[34] The buffering capacity of the gas–aerosol system, defined as the amount of acidic or basic species necessary to change pH_i by 1 unit, increases with $[NH_{3(g)}]$ ($\partial pH_i/\partial[NH_{3(g)}] \approx 0.4/[NH_{3(g)}]$). $a_{NH^+_{4(aq)}}$ is a function of RH and is also affected by aerosol composition (ions coexisting in the aqueous phase). We show, in the SI, that the sensitivities of pH_i to these variables are consistent between Equation (4) and thermodynamic models. This simple buffer equation can help understand the influence of different meteorological and chemical factors on the pH_i estimated by thermodynamic modeling.

As shown in Figure 4, the mean (± standard error) pH_i modeled by ISORROPIA were 4.52 ± 0.02, 4.73 ± 0.05, 4.77 ± 0.03, and 4.89 ± 0.04 for the winters of 2014/2015, 2016/2017, 2017/2018, and 2018/2019, respectively. The differences between 2014/2015 and 2016/2017 and between

2017/2018 and 2018/2019 were statistically significant ($p < 0.05$ from the Mann–Whitney U test), whereas that between 2016/2017 and 2017/2018 was insignificant. Note that only data for RH > 60% were considered when PM_1 was liquid. The bias in pH_i owing to the T difference was removed. An increase of 0.37 ± 0.05 unit from 2014/2015 to 2018/2019 was estimated in the modeled pH_i by ISORROPIA, agreeing well with the pH_i increase of about 0.4 unit modeled by E-AIM (Figure 4b). Although both models suggested a similar increase in pH_i, a systematic difference existed in their modeled pH_i, probably arising from different treatments of hydrogen ion activity coefficient ($\gamma_{H^+_{(aq)}}$) and bisulfate ion dissociation.[33,78]

The modeled pH_i increases of 0.3–0.4 unit from 2014/2015 to 2018/2019 could be explained by changes in $[NH_{3(g)}]$ and $a_{NH^+_{4(aq)}}$. $\log_{10}([NH_{3(g)}])$ increased by about 0.3 during this time period. The changes in aerosol composition (more nitrate and less sulfate and chloride) led to a minor decrease in $\gamma_{NH^+_{4(aq)}}$ and thus increased pH_i by about 0.1 unit (Figure S6). It was noted that our thermodynamic calculations used the total (gas + aerosol) measurements of semivolatile species as inputs and allowed them to be repartitioned between the two phases. If aerosol measurements of chemical species were not charge balanced, which was common given the various uncertainties in sampling and chemical analyses, the modeled and measured $[NH_{3(g)}]$ might differ due to its repartitioning (for achieving the charge balance in the modeled aerosol phase), introducing an additional bias in the modeled pH_i. The largest disagreement occurred in 2014/2015 winter when ISORROPIA underpredicted $[NH_{3(g)}]$ by about 20% compared with the measurements (Figure S1). A sensitivity calculation showed that the disagreement in 2014/2015 implied a possible bias in the modeled pH_i by about 0.1 unit.

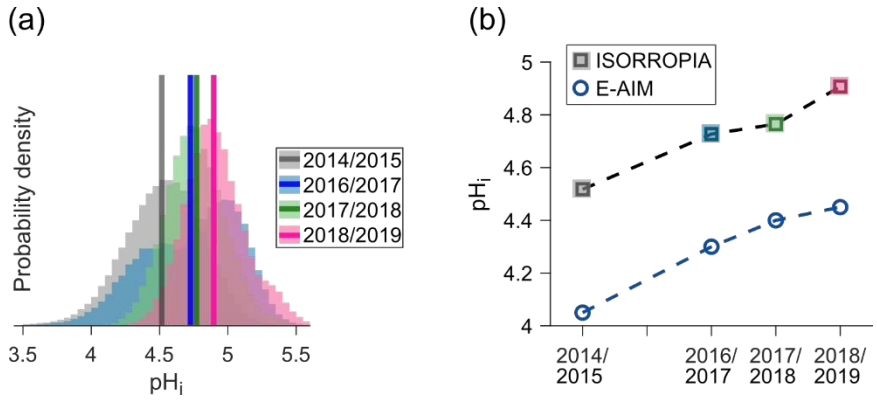

Figure 4. (a) shows the mean values and probability density distributions of aerosol pH_i modeled by ISORROPIA in recent winters. (b) presents the mean pH_i calculated from both ISORROPIA and E-AIM. Data were obtained under high RH condition (> 60%).

In summary, this study provides two new findings for Beijing winter haze events which are associated with high RH. First, the water-uptake ability of inorganic aerosols, characterized by the modeled G_{mi}, declined by about 9%–17% during the four seasons (from 2014/2015 to 2018/2019) due to changes in aerosol chemical composition. Nitrate has become the primary species to uptake aerosol water. Second, inorganic aerosol acidity, characterized by the modeled pH_i which increased by about 0.3–0.4 unit during this time period, also declined mainly as a response to rising ammonia. There are several limitations and assumptions in this work. First, the thermodynamic calculations conducted here assumed internally mixed inorganic aerosols and phase equilibrium. Second, the acidity of organic aerosol phase was not investigated.[79] The water content associated with organics estimated by the κ-Köhler theory[80] was about a factor of 5 lower than that with inorganics in Beijing winter haze.[33] Third, minor water-soluble aerosol species, primarily including nonvolatile cations and hydrophilic organic acid salts, were unavailable in our measurements. Accordingly, two sensitivity calculations were conducted (details in the SI) using the available data measured under Beijing winter haze conditions by previous studies, and their

295 results suggested that the finding of declined acidity and water uptake remained when considering
296 nonvolatile cations and hydrophilic organic acids.

297 The findings of this study have two implications. First, there are either positive or negative
298 chemical feedbacks in secondary aerosol production. On one hand, the declining aerosol water
299 uptake implies that the volume for heterogenous processes to occur has become smaller during
300 recent winter seasons. On the other hand, heterogeneous chemical reactions may be enhanced or
301 inhibited by declining aerosol acidity (i.e., rising aerosol pH).[9] Examples include nitrate photolysis
302 and subsequent HONO/NO_2^- production,[81] organosulfates (OSs) and nitrooxy-Oss formation,[82,83]
303 and the oxidation of $SO_{2(aq)}$ (the sum of $SO_2{\cdot}H_2O$, HSO_3^-, and SO_3^{2-}) by NO_2, O_3, and transition
304 metals + O_2.[10] The increase of 0.3 unit in the modeled pH from 2014/2015 to 2018/2019 winter
305 translated to a halved $a_{H^+_{(aq)}}$. A calculation following Shao et al. (2019)[18] suggested that these two
306 factors together could have led to large increases in the *in-situ* oxidation rates of $SO_{2(aq)}$ by O_3
307 (+240%) and NO_2 (+70%) whereas a significant decrease in the oxidation rate by transition metals
308 + O_2 (−90%). Note in this calculation that the other factors (e.g., the reactant concentrations in the
309 aqueous phase) were assumed to remain the same in order to isolate the effects of aerosol water
310 uptake and acidity. The O_3 and NO_2 pathways responded positively to pH because the solubility
311 of $SO_{2(aq)}$ increased at higher pH and because the equilibrium among $SO_2{\cdot}H_2O$, HSO_3^-, and SO_3^{2-}
312 shifted with changed pH.[74] The change in the O_3 reaction pathway than the NO_2 pathway since O_3
313 mainly reacted with SO_3^{2-} while NO_2 reacted with HSO_3^-.[10] The negative response of the transition
314 metals + O_2 pathway arose partly from the high solubility of Fe^{3+} and Mn^{2+} at low pH.[18] Chemical
315 feedbacks may help explain the observed slower declines in sulfate relative to SO_2 for winter haze
316 during recent years. The sulfate/SO_2 ratios in 2018/2019 increased by about 80% compared to the
317 ratios in 2014/2015 and by over a factor of 2 when compared to 2011/2012 (data from ref[66]) (Figure

318 S7). Since almost all the sulfate is converted by SO_2,[11] the enhanced sulfate/SO_2 ratios imply that
319 the oxidation of SO_2 may have become more efficient. As shown earlier, the rates of SO_2 oxidation
320 in aerosol water by O_3 and NO_2 increased as a result of declined aerosol acidity. Chemical transport
321 modeling studies should be conducted to investigate the contributions of different SO_2 oxidation
322 pathways and the role of meteorology. A better characterization of the mechanisms responsible for
323 SO_2 oxidation can help evaluate the effects of the past (and future) emission mitigation efforts.
324 The second implication is that reducing NH_3 emissions may have become less effective than
325 before as a measure to alleviate Beijing winter haze pollution.[84] The buffering capacity of the gas-
326 particle system have increased due to rising NH_3. It should be noted that NH_3 emissions in North
327 China, especially in urban areas, remain poorly quantified and the contributions of different
328 sources are subject to debate. Some studies[85-89] have argued that slip of NH_3 (due to urea used in
329 the selective catalytic reduction (SCR) systems) from industrial or power generation plants and
330 evasion from green space are important or even dominant sources to atmospheric NH_3 in urban
331 areas. Fossil fuel combustion and biomass burning were also suggested to be potential sources.[90,91]
332 Others[92-94] have argued that NH_3 is dominated by agricultural activities (due to volatilization from
333 fertilizer and livestock waste). An additional factor hindering our understanding is that the current
334 estimates of agricultural NH_3 emissions in China may differ by a factor of 2.[94] The reason for
335 rising NH_3 has also been poorly investigated. Liu et al. (2018)[39] studied satellite observations of
336 NH_3 columns and concluded that more rapid reductions in emissions of SO_2 and NO_x compared to
337 NH_3 led to an increase in tropospheric NH_3 columns over the North China Plain since 2013. The
338 Multi-resolution Emission Inventory for China[38] showed, during 2013–2017, that emissions of
339 SO_2, NO_x, and NH_3 decreased by 65%, 20%, and 4%, respectively. Note that a few non-agricultural
340 sources of NH_3 (e.g., slip) were not included in the inventory. The increasing penetration rates of

SCR systems in power plants (50% in 2013 and 95% in 2017)[38,95] may imply an increase in NH_3 slip. Therefore, future research efforts need to be undertaken to quantify NH_3 sources and driving factors. From the perspective of thermodynamics and based on gas/aerosol measurement data, this study suggests that a substantial (> 50%) NH_3 emission reduction is necessary to effectively reduce inorganic aerosol mass under the present Beijing winter haze conditions.

ASSOCIATED CONTENT

Supporting Information

The Supporting Information is available free of charge on the ACS Publications website at DOI: 00.0000/acs.000.0000000. Additional data, figures, and tables, some of which are referenced directly within the manuscript. Also included are detailed descriptions of field measurements and derivations of the buffer equation.

AUTHOR INFORMATION

Corresponding Author

S.W. (E-mail: shxwang@tsinghua.edu.cn), Y.S. (E-mail: sunyele@mail.iap.ac.cn), and B.L. (E-mail: liubaoxian28@163.com)

Notes

The authors declare no competing financial interest.

ACKNOWLEDGMENTS

This publication was made possible by funding from the Harvard Global Institute and the National Natural Science Foundation of China (21625701 and 91744207). We thank Simon Clegg for helpful discussions on the E-AIM model.

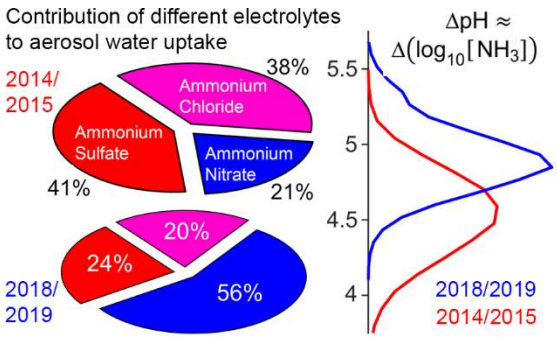

TOC Art

REFERENCES

(1) Nguyen, T. K. V.; Zhang, Q.; Jimenez, J. L.; Pike, M.; Carlton, A. G. Liquid water: ubiquitous contributor to aerosol mass. *Environ. Sci. Technol. Lett.* **2016,** *3*, 257-263.

(2) Pilinis, C.; Seinfeld, J. H.; Grosjean, D. Water content of atmospheric aerosols. *Atmos. Environ.* **1989,** *23*, 1601-1606.

(3) Guo, H.; Xu, L.; Bougiatioti, A.; Cerully, K. M.; Capps, S. L.; Hite Jr, J. R.; Carlton, A. G.; Lee, S. H.; Bergin, M. H.; Ng, N. L.; Nenes, A.; Weber, R. J. Fine-particle water and pH in the southeastern United States. *Atmos. Chem. Phys.* **2015,** *15*, 5211-5228.

(4) Malm, W. C.; Day, D. E. Estimates of aerosol species scattering characteristics as a function of relative humidity. *Atmos. Environ.* **2001,** *35*, 2845-2860.

(5) Martin, S. T.; Hung, H. M.; Park, R. J.; Jacob, D. J.; Spurr, R. J. D.; Chance, K. V.; Chin, M. Effects of the physical state of tropospheric ammonium-sulfate-nitrate particles on global aerosol direct radiative forcing. *Atmos. Chem. Phys.* **2004,** *4*, 183-214.

(6) Nah, T.; Guo, H.; Sullivan, A. P.; Chen, Y.; Tanner, D. J.; Nenes, A.; Russell, A.; Ng, N. L.; Huey, L. G.; Weber, R. J. Characterization of aerosol composition, aerosol acidity, and organic acid partitioning at an agriculturally intensive rural southeastern US site. *Atmos. Chem. Phys.* **2018,** *18*, 11471-11491.

(7) Alexander, B.; Park, R. J.; Jacob, D. J.; Li, Q. B.; Yantosca, R. M.; Savarino, J.; Lee, C. C. W.; Thiemens, M. H. Sulfate formation in sea-salt aerosols: Constraints from oxygen isotopes. *J. Geophys. Res. Atmos.* **2005,** *110*.

(8) Thornton, J. A.; Braban, C. F.; Abbatt, J. P. D. N_2O_5 hydrolysis on sub-micron organic aerosols: the effect of relative humidity, particle phase, and particle size. *Phys. Chem. Chem. Phys.* **2003,** *5*, 4593-4603.

(9) Ravishankara, A. R. Heterogeneous and multiphase chemistry in the troposphere. *Science* **1997,** *276*, 1058-1065.

(10) Cheng, Y.; Zheng, G.; Wei, C.; Mu, Q.; Zheng, B.; Wang, Z.; Gao, M.; Zhang, Q.; He, K.; Carmichael, G.; Pöschl, U.; Su, H. Reactive nitrogen chemistry in aerosol water as a source of sulfate during haze events in China. *Sci. Adv.* **2016,** *2*, e1601530.

(11) Wang, G.; Zhang, R.; Gomez, M. E.; Yang, L.; Levy Zamora, M.; Hu, M.; Lin, Y.; Peng, J.; Guo, S.; Meng, J.; Li, J.; Cheng, C.; Hu, T.; Ren, Y.; Wang, Y.; Gao, J.; Cao, J.; An, Z.; Zhou, W.; Li, G.; Wang, J.; Tian, P.; Marrero-Ortiz, W.; Secrest, J.; Du, Z.; Zheng, J.; Shang, D.; Zeng, L.; Shao, M.; Wang, W.; Huang, Y.; Wang, Y.; Zhu, Y.; Li, Y.; Hu, J.; Pan, B.; Cai, L.; Cheng, Y.; Ji, Y.; Zhang, F.; Rosenfeld, D.; Liss, P. S.; Duce, R. A.; Kolb, C. E.; Molina, M. J. Persistent sulfate formation from London Fog to Chinese haze. *Proc. Natl. Acad. Sci. U. S. A.* **2016,** *113*, 13630-13635.

(12) Wu, Z.; Wang, Y.; Tan, T.; Zhu, Y.; Li, M.; Shang, D.; Wang, H.; Lu, K.; Guo, S.; Zeng, L.; Zhang, Y. Aerosol liquid water driven by anthropogenic inorganic salts: Implying its key role in haze formation over the North China Plain. *Environ. Sci. Technol. Lett.* **2018,** *5*, 160-166.

(13) Gao, J.; Woodward, A.; Vardoulakis, S.; Kovats, S.; Wilkinson, P.; Li, L.; Xu, L.; Li, J.; Yang, J.; Li, J.; Cao, L.; Liu, X.; Wu, H.; Liu, Q. Haze, public health and mitigation measures in China: A review of the current evidence for further policy response. *Sci. Total Environ.* **2017,** *578*, 148-157.

(14) Liu, Y.; Wu, Z.; Wang, Y.; Xiao, Y.; Gu, F.; Zheng, J.; Tan, T.; Shang, D.; Wu, Y.; Zeng, L.; Hu, M.; Bateman, A. P.; Martin, S. T. Submicrometer particles are in the liquid state during heavy haze episodes in the urban atmosphere of Beijing, China. *Environ. Sci. Technol. Lett.* **2017,** *4*, 427-432.

(15) Gen, M.; Zhang, R.; Huang, D. D.; Li, Y.; Chan, C. K. Heterogeneous SO_2 oxidation in sulfate formation by photolysis of particulate nitrate. *Environ. Sci. Technol. Lett.* **2019,** *6*, 86-91.

(16) Hung, H.-M.; Hsu, M.-N.; Hoffmann, M. R. Quantification of SO_2 oxidation on interfacial surfaces of acidic micro-droplets: Implication for ambient sulfate formation. *Environ. Sci. Technol.* **2018,** *52*, 9079-9086.

(17) Li, L.; Hoffmann, M. R.; Colussi, A. J. Role of nitrogen dioxide in the production of sulfate during Chinese haze-aerosol episodes. *Environ. Sci. Technol.* **2018,** *52*, 2686-2693.

(18) Shao, J.; Chen, Q.; Wang, Y.; Lu, X.; He, P.; Sun, Y.; Shah, V.; Martin, R. V.; Philip, S.; Song, S.; Zhao, Y.; Xie, Z.; Zhang, L.; Alexander, B. Heterogeneous sulfate aerosol formation mechanisms during wintertime Chinese haze events: air quality model assessment using observations of sulfate oxygen isotopes in Beijing. *Atmos. Chem. Phys.* **2019,** *19*, 6107-6123.

(19) Nguyen, T. K. V.; Petters, M. D.; Suda, S. R.; Guo, H.; Weber, R. J.; Carlton, A. G. Trends in particle-phase liquid water during the Southern Oxidant and Aerosol Study. *Atmos. Chem. Phys.* **2014,** *14*, 10911-10930.

(20) Rader, D. J.; McMurry, P. H. Application of the tandem differential mobility analyzer to studies of droplet growth or evaporation. *J. Aerosol Sci.* **1986,** *17*, 771-787.

(21) Fountoukis, C.; Nenes, A. ISORROPIA II: a computationally efficient thermodynamic equilibrium model for K^+-Ca^{2+}-Mg^{2+}-NH_4^+-Na^+-SO_4^{2-}-NO_3^--Cl^--H_2O aerosols. *Atmos. Chem. Phys.* **2007,** *7*, 4639-4659.

(22) Wexler, A. S.; Clegg, S. L. Atmospheric aerosol models for systems including the ions H^+, NH_4^+, Na^+, SO_4^{2-}, NO_3^-, Cl^-, Br^-, and H_2O. *J. Geophys. Res. Atmos.* **2002,** *107*.

(23) Tan, H.; Cai, M.; Fan, Q.; Liu, L.; Li, F.; Chan, P. W.; Deng, X.; Wu, D. An analysis of aerosol liquid water content and related impact factors in Pearl River Delta. *Sci. Total Environ.* **2017,** *579*, 1822-1830.

(24) Freedman, M. A.; Ott, E.-J. E.; Marak, K. E. Role of pH in aerosol processes and measurement challenges. *J. Phys. Chem. A* **2019,** *123*, 1275-1284.

(25) Wei, H.; Vejerano, E. P.; Leng, W.; Huang, Q.; Willner, M. R.; Marr, L. C.; Vikesland, P. J. Aerosol microdroplets exhibit a stable pH gradient. *Proc. Natl. Acad. Sci. U. S. A.* **2018,** *115*, 7272-7277.

(26) Craig, R. L.; Peterson, P. K.; Nandy, L.; Lei, Z.; Hossain, M. A.; Camarena, S.; Dodson, R. A.; Cook, R. D.; Dutcher, C. S.; Ault, A. P. Direct determination of aerosol pH: size-resolved measurements of submicrometer and supermicrometer aqueous particles. *Anal. Chem.* **2018,** *90*, 11232-11239.

(27) Wang, Y.; Yao, L.; Wang, L.; Liu, Z.; Ji, D.; Tang, G.; Zhang, J.; Sun, Y.; Hu, B.; Xin, J. Mechanism for the formation of the January 2013 heavy haze pollution episode over central and eastern China. *Sci. China Earth Sci.* **2014,** *57*, 14-25.

(28) Wang, X.; Wang, W.; Yang, L.; Gao, X.; Nie, W.; Yu, Y.; Xu, P.; Zhou, Y.; Wang, Z. The secondary formation of inorganic aerosols in the droplet mode through heterogeneous aqueous reactions under haze conditions. *Atmos. Environ.* **2012,** *63*, 68-76.

(29) Sun, Y.; Chen, C.; Zhang, Y.; Xu, W.; Zhou, L.; Cheng, X.; Zheng, H.; Ji, D.; Li, J.; Tang, X.; Fu, P.; Wang, Z. Rapid formation and evolution of an extreme haze episode in Northern China during winter 2015. *Sci. Rep.* **2016,** *6*, 27151.

(30) Shi, G.; Xu, J.; Peng, X.; Xiao, Z.; Chen, K.; Tian, Y.; Guan, X.; Feng, Y.; Yu, H.; Nenes, A.; Russell, A. G. pH of aerosols in a polluted atmosphere: Source contributions to highly acidic aerosol. *Environ. Sci. Technol.* **2017,** *51*, 4289-4296.

(31) He, P.; Alexander, B.; Geng, L.; Chi, X.; Fan, S.; Zhan, H.; Kang, H.; Zheng, G.; Cheng, Y.; Su, H.; Liu, C.; Xie, Z. Isotopic constraints on heterogeneous sulfate production in Beijing haze. *Atmos. Chem. Phys.* **2018,** *18*, 5515-5528.

(32) Liu, M.; Song, Y.; Zhou, T.; Xu, Z.; Yan, C.; Zheng, M.; Wu, Z.; Hu, M.; Wu, Y.; Zhu, T. Fine particle pH during severe haze episodes in northern China. *Geophys. Res. Lett.* **2017,** *44*, 5213-5221.

(33) Song, S.; Gao, M.; Xu, W.; Shao, J.; Shi, G.; Wang, S.; Wang, Y.; Sun, Y.; McElroy, M. B. Fine-particle pH for Beijing winter haze as inferred from different thermodynamic equilibrium models. *Atmos. Chem. Phys.* **2018,** *18*, 7423-7438.

(34) Guo, H.; Weber, R. J.; Nenes, A. High levels of ammonia do not raise fine particle pH sufficiently to yield nitrogen oxide-dominated sulfate production. *Sci. Rep.* **2017,** *7*, 12109.

(35) Tan, T.; Hu, M.; Li, M.; Guo, Q.; Wu, Y.; Fang, X.; Gu, F.; Wang, Y.; Wu, Z. New insight into $PM_{2.5}$ pollution patterns in Beijing based on one-year measurement of chemical compositions. *Sci. Total Environ.* **2018,** *621*, 734-743.

(36) Zhao, M.; Wang, S.; Tan, J.; Hua, Y.; Wu, D.; Hao, J. Variation of urban atmospheric ammonia pollution and its relation with $PM_{2.5}$ chemical property in winter of Beijing, China. *Aerosol Air Qual. Res.* **2016,** *16*, 1378-1389.

(37) Silver, B.; Reddington, C. L.; Arnold, S. R.; Spracklen, D. V. Substantial changes in air pollution across China during 2015–2017. *Environ. Res. Lett.* **2018,** *13*, 114012.

(38) Zheng, B.; Tong, D.; Li, M.; Liu, F.; Hong, C.; Geng, G.; Li, H.; Li, X.; Peng, L.; Qi, J.; Yan, L.; Zhang, Y.; Zhao, H.; Zheng, Y.; He, K.; Zhang, Q. Trends in China's anthropogenic emissions since 2010 as the consequence of clean air actions. *Atmos. Chem. Phys.* **2018,** *18*, 14095-14111.

(39) Liu, M.; Huang, X.; Song, Y.; Xu, T.; Wang, S.; Wu, Z.; Hu, M.; Zhang, L.; Zhang, Q.; Pan, Y.; Liu, X.; Zhu, T. Rapid SO_2 emission reductions significantly increase tropospheric ammonia concentrations over the North China Plain. *Atmos. Chem. Phys.* **2018,** *18*, 17933-17943.

(40) Shao, P.; Tian, H.; Sun, Y.; Liu, H.; Wu, B.; Liu, S.; Liu, X.; Wu, Y.; Liang, W.; Wang, Y.; Gao, J.; Xue, Y.; Bai, X.; Liu, W.; Lin, S.; Hu, G. Characterizing remarkable changes of severe haze events and chemical compositions in multi-size airborne particles (PM_1, $PM_{2.5}$ and PM_{10}) from January 2013 to 2016–2017 winter in Beijing, China. *Atmos. Environ.* **2018,** *189*, 133-144.

(41) Li, K.; Jacob, D. J.; Liao, H.; Shen, L.; Zhang, Q.; Bates, K. H. Anthropogenic drivers of 2013–2017 trends in summer surface ozone in China. *Proc. Natl. Acad. Sci. U. S. A.* **2019,** *116*, 422-427.

(42) Li, H.; Cheng, J.; Zhang, Q.; Zheng, B.; Zhang, Y.; Zheng, G.; He, K. Rapid transition in winter aerosol composition in Beijing from 2014 to 2017: response to clean air actions. *Atmos. Chem. Phys.* **2019,** *19*, 11485-11499.

(43) Zhai, S.; Jacob, D. J.; Wang, X.; Shen, L.; Li, K.; Zhang, Y.; Gui, K.; Zhao, T.; Liao, H. Fine particulate matter ($PM_{2.5}$) trends in China, 2013-2018: separating contributions from anthropogenic emissions and meteorology. *Atmos. Chem. Phys.* **2019,** *19*, 11031-11041.

(44) Weber, R. J.; Guo, H.; Russell, A. G.; Nenes, A. High aerosol acidity despite declining atmospheric sulfate concentrations over the past 15 years. *Nat. Geosci.* **2016,** *9*, 282.

(45) Tao, Y.; Murphy, J. G. The sensitivity of $PM_{2.5}$ acidity to meteorological parameters and chemical composition changes: 10-year records from six Canadian monitoring sites. *Atmos. Chem. Phys.* **2019,** *19*, 9309–9320.

(46) Lawal, A. S.; Guan, X.; Liu, C.; Henneman, L. R. F.; Vasilakos, P.; Bhogineni, V.; Weber, R. J.; Nenes, A.; Russell, A. G. Linked response of aerosol acidity and ammonia to SO_2 and NO_x emissions reductions in the United States. *Environ. Sci. Technol.* **2018,** *52*, 9861-9873.

(47) Guo, H.; Nenes, A.; Weber, R. J. The underappreciated role of nonvolatile cations in aerosol ammonium-sulfate molar ratios. *Atmos. Chem. Phys.* **2018,** *18*, 17307-17323.

(48) Vasilakos, P.; Russell, A.; Weber, R.; Nenes, A. Understanding nitrate formation in a world with less sulfate. *Atmos. Chem. Phys.* **2018,** *18*, 12765-12775.

(49) Shah, V.; Jaeglé, L.; Thornton, J. A.; Lopez-Hilfiker, F. D.; Lee, B. H.; Schroder, J. C.; Campuzano-Jost, P.; Jimenez, J. L.; Guo, H.; Sullivan, A. P.; Weber, R. J.; Green, J. R.; Fiddler, M. N.; Bililign, S.; Campos, T. L.; Stell, M.; Weinheimer, A. J.; Montzka, D. D.; Brown, S. S. Chemical feedbacks

weaken the wintertime response of particulate sulfate and nitrate to emissions reductions over the eastern United States. *Proc. Natl. Acad. Sci. U. S. A.* **2018,** *115*, 8110-8115.

(50) Battaglia, M. A.; Douglas, S.; Hennigan, C. J. Effect of the urban heat island on aerosol pH. *Environ. Sci. Technol.* **2017,** *51*, 13095-13103.

(51) Jia, S.; Wang, X.; Zhang, Q.; Sarkar, S.; Wu, L.; Huang, M.; Zhang, J.; Yang, L. Technical note: Comparison and interconversion of pH based on different standard states for aerosol acidity characterization. *Atmos. Chem. Phys.* **2018,** *18*, 11125-11133.

(52) Fountoukis, C.; Nenes, A.; Sullivan, A.; Weber, R.; Van Reken, T.; Fischer, M.; Matías, E.; Moya, M.; Farmer, D.; Cohen, R. C. Thermodynamic characterization of Mexico City aerosol during MILAGRO 2006. *Atmos. Chem. Phys.* **2009,** *9*, 2141-2156.

(53) Xu, W.; Sun, Y.; Wang, Q.; Zhao, J.; Wang, J.; Ge, X.; Xie, C.; Zhou, W.; Du, W.; Li, J.; Fu, P.; Wang, Z.; Worsnop, D. R.; Coe, H. Changes in aerosol chemistry from 2014 to 2016 in winter in Beijing: Insights from high-resolution aerosol mass spectrometry. *J. Geophys. Res. Atmos.* **2019,** *124*, 1132-1147.

(54) Bertram, A. K.; Martin, S. T.; Hanna, S. J.; Smith, M. L.; Bodsworth, A.; Chen, Q.; Kuwata, M.; Liu, A.; You, Y.; Zorn, S. R. Predicting the relative humidities of liquid-liquid phase separation, efflorescence, and deliquescence of mixed particles of ammonium sulfate, organic material, and water using the organic-to-sulfate mass ratio of the particle and the oxygen-to-carbon elemental ratio of the organic component. *Atmos. Chem. Phys.* **2011,** *11*, 10995-11006.

(55) Song, M.; Marcolli, C.; Krieger, U. K.; Zuend, A.; Peter, T. Liquid-liquid phase separation in aerosol particles: Dependence on O:C, organic functionalities, and compositional complexity. *Geophys. Res. Lett.* **2012,** *39*.

(56) Nenes, A.; Pandis, S. N.; Pilinis, C. ISORROPIA: A New Thermodynamic Equilibrium Model for Multiphase Multicomponent Inorganic Aerosols. *Aquat. Geochem.* **1998,** *4*, 123-152.

(57) Stokes, R. H.; Robinson, R. A. Interactions in aqueous nonelectrolyte solutions. I. solute-solvent equilibria. *J. Phys. Chem.* **1966,** *70*, 2126-2131.

(58) Zdanovskii, A. B. New methods for calculating solubilities of electrolytes in multicomponent systems. *Zh. Fiz. Khim.* **1948,** *22*, 1475-1485.

(59) Zhang, Y.; Seigneur, C.; Seinfeld, J. H.; Jacobson, M.; Clegg, S. L.; Binkowski, F. S. A comparative review of inorganic aerosol thermodynamic equilibrium modules: similarities, differences, and their likely causes. *Atmos. Environ.* **2000,** *34*, 117-137.

(60) Zaveri, R. A.; Easter, R. C.; Peters, L. K. A computationally efficient Multicomponent Equilibrium Solver for Aerosols (MESA). *J. Geophys. Res. Atmos.* **2005,** *110*.

(61) Topping, D. O.; McFiggans, G. B.; Coe, H. A curved multi-component aerosol hygroscopicity model framework: Part 1 – Inorganic compounds. *Atmos. Chem. Phys.* **2005,** *5*, 1205-1222.

(62) Jacobson, M. Z. Studying the effects of calcium and magnesium on size-distributed nitrate and ammonium with EQUISOLV II. *Atmos. Environ.* **1999,** *33*, 3635-3649.

(63) Hennigan, C. J.; Izumi, J.; Sullivan, A. P.; Weber, R. J.; Nenes, A. A critical evaluation of proxy methods used to estimate the acidity of atmospheric particles. *Atmos. Chem. Phys.* **2015,** *15*, 2775-2790.

(64) Friese, E.; Ebel, A. Temperature dependent thermodynamic model of the system H^+–NH_4^+–Na^+–SO_4^{2-}–NO_3^-–Cl^-–H_2O. *J. Phys. Chem. A* **2010,** *114*, 11595-11631.

(65) Wang, Y.; Zhang, Q.; Jiang, J.; Zhou, W.; Wang, B.; He, K.; Duan, F.; Zhang, Q.; Philip, S.; Xie, Y. Enhanced sulfate formation during China's severe winter haze episode in January 2013 missing from current models. *J. Geophys. Res. Atmos.* **2014,** *119*, 10425-10440.

(66) Sun, Y.; Wang, Z.; Fu, P.; Jiang, Q.; Yang, T.; Li, J.; Ge, X. The impact of relative humidity on aerosol composition and evolution processes during wintertime in Beijing, China. *Atmos. Environ.* **2013,** *77*, 927-934.

(67) Li, G.; Bei, N.; Cao, J.; Huang, R.; Wu, J.; Feng, T.; Wang, Y.; Liu, S.; Zhang, Q.; Tie, X.; Molina, L. T. A possible pathway for rapid growth of sulfate during haze days in China. *Atmos. Chem. Phys.* **2017,** *17*, 3301-3316.

(68) Ye, C.; Liu, P.; Ma, Z.; Xue, C.; Zhang, C.; Zhang, Y.; Liu, J.; Liu, C.; Sun, X.; Mu, Y. High H_2O_2 concentrations observed during haze periods during the winter in Beijing: Importance of H_2O_2 oxidation in sulfate formation. *Environ. Sci. Technol. Lett.* **2018,** *5*, 757-763.

(69) Li, H.; Zhang, Q.; Zhang, Q.; Chen, C.; Wang, L.; Wei, Z.; Zhou, S.; Parworth, C.; Zheng, B.; Canonaco, F.; Prévôt, A. S. H.; Chen, P.; Zhang, H.; Wallington, T. J.; He, K. Wintertime aerosol chemistry and haze evolution in an extremely polluted city of the North China Plain: significant contribution from coal and biomass combustion. *Atmos. Chem. Phys.* **2017,** *17*, 4751-4768.

(70) Cheng, N.; Cheng, B.; Li, S.; Ning, T. Effects of meteorology and emission reduction measures on air pollution in Beijing during heating seasons. *Atmos. Pollut. Res.* **2019,** *10*, 971-979.

(71) Cheng, J.; Su, J.; Cui, T.; Li, X.; Dong, X.; Sun, F.; Yang, Y.; Tong, D.; Zheng, Y.; Li, Y.; Li, J.; Zhang, Q.; He, K. Dominant role of emission reduction in PM2.5 air quality improvement in Beijing during 2013–2017: a model-based decomposition analysis. *Atmos. Chem. Phys.* **2019,** *19*, 6125-6146.

(72) Chen, Z.; Chen, D.; Wen, W.; Zhuang, Y.; Kwan, M. P.; Chen, B.; Zhao, B.; Yang, L.; Gao, B.; Li, R.; Xu, B. Evaluating the "2+26" regional strategy for air quality improvement during two air pollution alerts in Beijing: variations in PM2.5 concentrations, source apportionment, and the relative contribution of local emission and regional transport. *Atmos. Chem. Phys.* **2019,** *19*, 6879-6891.

(73) Rood, M. J.; Shaw, M. A.; Larson, T. V.; Covert, D. S. Ubiquitous nature of ambient metastable aerosol. *Nature* **1989,** *337*, 537-539.

(74) Seinfeld, J. H.; Pandis, S. N., *Atmospheric chemistry and physics: from air pollution to climate change*. Third ed.; John Wiley & Sons, Inc.: Hoboken, New Jersey, 2016.

(75) Clegg, S. L.; Brimblecombe, P.; Wexler, A. S. Thermodynamic model of the system H^+–NH_4^+–Na^+–SO_4^{2-}–NO_3^-–Cl^-–H_2O at 298.15 K. *J. Phys. Chem. A* **1998,** *102*, 2155-2171.

(76) Clegg, S. L.; Brimblecombe, P.; Wexler, A. S. Thermodynamic model of the system H^+–NH_4^+–SO_4^{2-}–NO_3^-–H_2O at tropospheric temperatures. *J. Phys. Chem. A* **1998,** *102*, 2137-2154.

(77) Po, H. N.; Senozan, N. M. The Henderson-Hasselbalch equation: its history and limitations. *J. Chem. Educ.* **2001,** *78*, 1499-1503.

(78) Peng, X.; Vasilakos, P.; Nenes, A.; Shi, G.; Qian, Y.; Shi, X.; Xiao, Z.; Chen, K.; Feng, Y.; Russell, A. G. Detailed analysis of estimated pH, activity coefficients, and ion concentrations between the three aerosol thermodynamic models. *Environ. Sci. Technol.* **2019,** *53*, 8903-8913.

(79) Battaglia Jr, M. A.; Weber, R. J.; Nenes, A.; Hennigan, C. J. Effects of water-soluble organic carbon on aerosol pH. *Atmos. Chem. Phys. Discuss.* **2019,** *2019*, 1-36.

(80) Petters, M. D.; Kreidenweis, S. M. A single parameter representation of hygroscopic growth and cloud condensation nucleus activity. *Atmos. Chem. Phys.* **2007,** *7*, 1961-1971.

(81) Gen, M.; Zhang, R.; Huang, D. D.; Li, Y.; Chan, C. K. Heterogeneous oxidation of SO_2 in sulfate production during nitrate photolysis at 300 nm: Effect of pH, relative humidity, irradiation intensity, and the presence of organic compounds. *Environ. Sci. Technol.* **2019,** *53*, 8757-8766.

(82) Wang, Y.; Hu, M.; Guo, S.; Wang, Y.; Zheng, J.; Yang, Y.; Zhu, W.; Tang, R.; Li, X.; Liu, Y.; Le Breton, M.; Du, Z.; Shang, D.; Wu, Y.; Wu, Z.; Song, Y.; Lou, S.; Hallquist, M.; Yu, J. The secondary formation of organosulfates under interactions between biogenic emissions and anthropogenic pollutants in summer in Beijing. *Atmos. Chem. Phys.* **2018,** *18*, 10693-10713.

(83) Wang, S.; Zhou, S.; Tao, Y.; Tsui, W. G.; Ye, J.; Yu, J. Z.; Murphy, J. G.; McNeill, V. F.; Abbatt, J. P. D.; Chan, A. W. H. Organic peroxides and sulfur dioxide in aerosol: Source of particulate sulfate. *Environ. Sci. Technol.* **2019,** *53*, 10695-10704.

(84) An, Z.; Huang, R.-J.; Zhang, R.; Tie, X.; Li, G.; Cao, J.; Zhou, W.; Shi, Z.; Han, Y.; Gu, Z.; Ji, Y. Severe haze in northern China: A synergy of anthropogenic emissions and atmospheric processes. *Proc. Natl. Acad. Sci. U. S. A.* **2019**.

(85) Hu, Q.; Yao, X. Reply to Comment on "identification of major sources of atmospheric NH_3 in an urban environment in northern China during wintertime". *Environ. Sci. Technol.* **2018,** *52*, 364-365.

(86) Pan, Y.; Tian, S.; Liu, D.; Fang, Y.; Zhu, X.; Gao, M.; Gao, J.; Michalski, G.; Wang, Y. Isotopic evidence for enhanced fossil fuel sources of aerosol ammonium in the urban atmosphere. *Environ. Pollut.* **2018,** *238*, 942-947.

(87) Pan, Y.; Tian, S.; Liu, D.; Fang, Y.; Zhu, X.; Zhang, Q.; Zheng, B.; Michalski, G.; Wang, Y. Fossil fuel combustion-related emissions dominate atmospheric ammonia sources during severe haze episodes: Evidence from 15N-stable isotope in size-resolved aerosol ammonium. *Environ. Sci. Technol.* **2016,** *50*, 8049-8056.

(88) Pan, Y.; Tian, S.; Liu, D.; Fang, Y.; Zhu, X.; Zhang, Q.; Zheng, B.; Michalski, G.; Wang, Y. Reply to Comment on "Fossil fuel combustion-related emissions dominate atmospheric ammonia sources during severe haze episodes: evidence from 15N-stable isotope in size-resolved aerosol ammonium". *Environ. Sci. Technol.* **2016,** *50*, 10767-10768.

(89) Teng, X.; Hu, Q.; Zhang, L.; Qi, J.; Shi, J.; Xie, H.; Gao, H.; Yao, X. Identification of major sources of atmospheric NH_3 in an urban environment in northern China during wintertime. *Environ. Sci. Technol.* **2017,** *51*, 6839-6848.

(90) Wang, Q.; Zhang, Q.; Ma, Z.; Ge, B.; Xie, C.; Zhou, W.; Zhao, J.; Xu, W.; Du, W.; Fu, P.; Lee, J.; Nemitz, E.; Cowan, N.; Mullinger, N.; Cheng, X.; Zhou, L.; Yue, S.; Wang, Z.; Sun, Y. Temporal characteristics and vertical distribution of atmospheric ammonia and ammonium in winter in Beijing. *Sci. Total Environ.* **2019,** *681*, 226-234.

(91) Sun, K.; Tao, L.; Miller, D. J.; Pan, D.; Golston, L. M.; Zondlo, M. A.; Griffin, R. J.; Wallace, H. W.; Leong, Y. J.; Yang, M. M.; Zhang, Y.; Mauzerall, D. L.; Zhu, T. Vehicle emissions as an important urban ammonia source in the United States and China. *Environ. Sci. Technol.* **2017,** *51*, 2472-2481.

(92) Chang, Y.; Ma, H. Comment on "Fossil fuel combustion-related emissions dominate atmospheric ammonia sources during severe haze episodes: Evidence from 15N-stable isotope in size-resolved aerosol ammonium". *Environ. Sci. Technol.* **2016,** *50*, 10765-10766.

(93) Zeng, Y.; Wang, S. Comment on "Identification of major sources of atmospheric NH_3 in an urban environment in northern China during wintertime". *Environ. Sci. Technol.* **2018,** *52*, 362-363.

(94) Zhang, L.; Chen, Y.; Zhao, Y.; Henze, D. K.; Zhu, L.; Song, Y.; Paulot, F.; Liu, X.; Pan, Y.; Lin, Y.; Huang, B. Agricultural ammonia emissions in China: reconciling bottom-up and top-down estimates. *Atmos. Chem. Phys.* **2018,** *18*, 339-355.

(95) Sun, W.; Shao, M.; Granier, C.; Liu, Y.; Ye, C. S.; Zheng, J. Y. Long-term trends of anthropogenic SO_2, NOx, CO, and NMVOCs emissions in China. *Earth's Future* **2018,** *6*, 1112-1133.